NeuroImage 178 (2018) 702–712

Contents lists available at ScienceDirect

NeuroImage

journal homepage: www.elsevier.com/locate/neuroimage

Cortical volume and sex influence visual gamma

Stan van Pelt [a,b], Elena Shumskaya [a,c], Pascal Fries [a,b,*]

[a] Donders Institute for Brain, Cognition and Behaviour, Radboud University Nijmegen, Kapittelweg 29, 6525 EN Nijmegen, The Netherlands
[b] Ernst Strüngmann Institute (ESI) for Neuroscience in Cooperation with Max Planck Society, Deutschordenstraße 46, 60528 Frankfurt, Germany
[c] Department of Human Genetics, Radboud University Medical Center, Nijmegen, The Netherlands

A B S T R A C T

Visually induced gamma–band activity (GBA) has been implicated in several central cognitive functions, in particular perceptual binding, the feedforward routing of attended stimulus information and memory encoding. Several studies have documented that the strength and frequency of GBA are influenced by both subject–intrinsic factors like age, and subject–extrinsic factors such as stimulus contrast. Here, we investigated the relative contributions of previously tested factors, additional factors, and their interactions, in a cohort of 158 subjects recorded with magnetoencephalography (MEG). In agreement with previous studies, we found that gamma strength and gamma peak frequency increase with stimulus contrast and stimulus velocity. Also in confirmation of previous findings, we report that gamma peak frequency declines with subject age. In addition, we found that gamma peak frequency is higher for subjects with thicker occipital cortex, but lower for larger occipital cortices. Also, gamma peak frequency is higher in female than male subjects. Extrinsic factors (stimulus contrast and velocity) and intrinsic factors (age, cortical thickness and sex) together explained 21% of the variance in gamma peak frequency and 20% of the variance in gamma strength. These results can contribute to our understanding of the mechanisms, by which gamma is generated, and the mechanisms, through which it affects the cognitive performance of a given individual subject.

Introduction

Gamma–band activity (30–90 Hz) plays a key role in cortical processing (Singer and Gray, 1995; Buzsáki and Wang, 2012; Fries, 2015). It is enhanced during perception and action (Fries et al., 2002; Wyart and Tallon–Baudry, 2008; Hoogenboom et al., 2010), selective attention (Fries et al., 2001; Bosman et al., 2012; Landau et al., 2015), and successful memory encoding (Howard et al., 2003; Fell et al., 2001). Interestingly, gamma frequency and amplitude are highly variable across human subjects, similar to cognitive functioning. The sources of gamma variability have been studied extensively over the last decade, but their relative contributions remain unclear. They can be organized along two dimensions: extrinsic factors, like stimuli and tasks, and intrinsic, subject–specific factors, like genetic makeup.

With regard to extrinsic factors, gamma amplitude and frequency increase for stimuli with increasing contrast (Hadjipapas et al., 2015) and increasing velocity (Swettenham et al., 2009). Conversely, gamma amplitude and frequency decrease with increasing stimulus eccentricity (van Pelt and Fries, 2013, but see Gregory et al., 2016). Stimulus size and spatial frequency have differential effects on gamma amplitude and frequency. Larger stimuli increase gamma strength (Gieselmann and Thiele, 2008; Perry et al., 2013), whereas they decrease gamma frequency (Gieselmann and Thiele, 2008; van Pelt and Fries, 2013) or leave it unaffected (Perry et al., 2013). Spatial frequency does not affect gamma frequency (van Pelt and Fries, 2013), but correlates positively (van Pelt and Fries, 2013) or via an inverted U–shape (Adjamian et al., 2004) with gamma amplitude.

Orthogonal to these extrinsic, stimulus–dependent factors, also intrinsic, subject–specific factors affect gamma amplitude and frequency. Both gamma frequency and amplitude are highly genetically determined (van Pelt et al., 2012), and they have a high test–retest reliability (Hoogenboom et al., 2006; Muthukumarashwamy et al., 2010). Gamma frequency decreases with age (Gaetz et al., 2012; Muthukumaraswamy et al., 2010, Robson et al., 2015). Effects of cortical size are yet inconclusive. Some studies report a positive correlation between gamma frequency and V1 size (but not with thickness or volume) (Schwarzkopf et al., 2012; Gregory et al., 2016), whereas others do not find such a relationship (Perry et al., 2013; Robson et al., 2015). Similarly equivocal findings exist for a possible correlation to cortical GABA levels (Muthukumarashwamy et al., 2009; Kujala et al., 2015; Cousijn et al., 2014; Robson et al., 2015).

Understanding the relative contributions of these factors and their interactions is crucial for a proper understanding of inter–individual differences in cognition. It will also provide further insights into the neurophysiological and potentially genetic mechanisms that underlie the gamma rhythm.

* Corresponding author. Ernst Strüngmann Institute for Neuroscience in Cooperation with Max Planck Society, Deutschordenstraße 46, 60528 Frankfurt, Germany.
E-mail addresses: stanvanpelt@gmail.com (S. van Pelt), pascal.fries@esi-frankfurt.de (P. Fries).

https://doi.org/10.1016/j.neuroimage.2018.06.005
Received 13 February 2018; Received in revised form 22 May 2018; Accepted 4 June 2018
Available online 5 June 2018

Here, we set out to systematically investigate the combined effects of both extrinsic and intrinsic factors on the gamma rhythm in a very large sample of healthy subjects, using magnetoencephalography (MEG) and structural magnetic resonance imaging (sMRI). One–hundred–and–fifty–eight subjects viewed a circular, moving grating, which they monitored to report a randomly timed change in velocity (van Pelt et al., 2012). Extrinsic stimulus factors were varied across trials, by using gratings at two different contrast levels, moving at three different velocities. Intrinsic factors, that were investigated, included sex and age of the subjects, as well as thickness, area, and volume of their occipital cortices.

Materials and methods

Experimental design and statistical analysis

Sample size and relevant subject-related information can be found in the *Subjects* section below. Data (pre)processing preceding the statistical analyses are described in the *MEG data analysis* section. Statistical analyses can be found in the *Results* section. Paired t-tests were used for within subject comparisons, and independent sample t-tests for between-group comparisons. Simple and multiple linear regressions were performed to compute correlational relations between factors. All inferential statistical tests were not repeated multiple times e.g. across frequency, thereby avoiding the need for corresponding corrections. Parts of the data have been used in two other studies to answer orthogonal research questions (Michalareas et al., 2016; van Ede et al., 2015).

Subjects

One–hundred–and–fifty–eight neurologically healthy subjects were recruited through the Radboud University participant database (radboud.sona–systems.com). Of all subjects, 106 were female (mean age 23.2y, SD 3.9) and 52 were male (mean age 24.3y, SD 4.4). All had normal or corrected–to–normal vision. The experiment was approved by the local ethics committee (Commissie mensgebonden onderzoek (CMO) regio Arnhem–Nijmegen, number 2001/095).

Experimental setup

Subjects were seated upright in a 275–channel whole–head magnetoencephalography (MEG) system (CTF systems, Canada) that was located in a magnetically shielded room (MSR). Bipolar electrodes were placed on four locations around the eyes: above and below the left eye, and at the outer side of both eyes. These respective vertical and horizontal electrooculargrams (EOG) were co–recorded with the MEG–signal for offline artifact detection. All data were recorded at 1200 Hz, and offline downsampled to 600 Hz. During the experiment, visual grating stimuli concentric to the fixation point (Fig. 1) were backprojected via two mirrors onto a translucent screen in front of the subject, using a Liquid-crystal display (LCD) projector (EIKI) that was located outside the MSR. Screen distance to the subject was 88 cm, projection dimensions were 45 × 34 cm (width x height), resolution 1024 × 768. The LCD projector updated the image at 60 Hz, and grating movement was implemented by changes occurring at each update. Note that the LCD operates differently from a conventional cathode ray tube (CRT) monitor. The CRT monitor produces a series of flashed images. By contrast, the LCD merely changes for each cycle the gray level of those pixels, that need to change e.g. to generate grating motion, and it does so with a relatively slow and thereby smooth dynamics. As the stimulus was a sine-wave grating, the gray-level changes per update, that generated grating movement, were very small, such that the stimulus contained minimal 60 Hz components. For the static grating, the LCD did not change at all. With these stimuli, including the static grating, we regularly observed gamma-band responses with relatively narrow peaks that did not center at 60 Hz. Examples of this can be seen for several stimulus conditions in Fig. 2A–C. These results strongly suggest that the visually induced gamma was not related to the 60 Hz update frequency of the LCD.

Paradigm and stimuli

Fig. 1 schematically illustrates the experimental paradigm. Each trial started with a fixation baseline of 1.5 s length, during which subjects fixated on a small, grayscale Gaussian dot. Subsequently, an inward-moving concentric grating was presented on a black background. After a variable amount of time, ranging between 0.75 and 3.0 s (determined by a hazard rate, see Hoogenboom et al., 2006), the stimulus increased velocity, which the subjects reported with a button press as quickly as possible. Hereafter, subjects received feedback on their performance (0.5 s), and the next trial started. The stimulus had a spatial frequency of 3 cycles per degree. It subtended 7 degrees of visual angle in diameter with a smooth taper at the edges.

The experiment consisted of four stimulus conditions. In three conditions, stimulus contrast was at 100%, while stimulus velocity was varied between 0.66 deg/s, 0.33 deg/s, and 0.0 deg/s (stationary). In the fourth condition, stimulus velocity was held at 0.66 deg/s, with stimulus contrast reduced to 50%. Thus, we varied the stimulus along one dimension, while keeping the other dimension at the value inducing strongest gamma, as found in previous studies and our own pilot recordings (Hadjipapas et al., 2015; Swettenham et al., 2009). Variations in velocity included two moving conditions, because the stationary

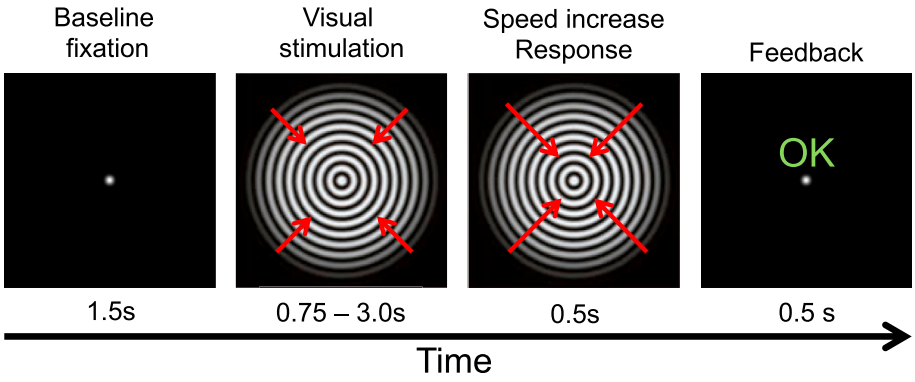

Fig. 1. Experimental paradigm. Each trial started with a 1.5 s baseline epoch, after which an inward-moving concentric grating was presented for a variable period between 0.6 and 3.0s. During this period, a stimulus velocity increase could occur, to which the subjects had to respond by pressing a response button. Hereafter, subjects recieved feedback on their performance (0.5s), and the next trial started.

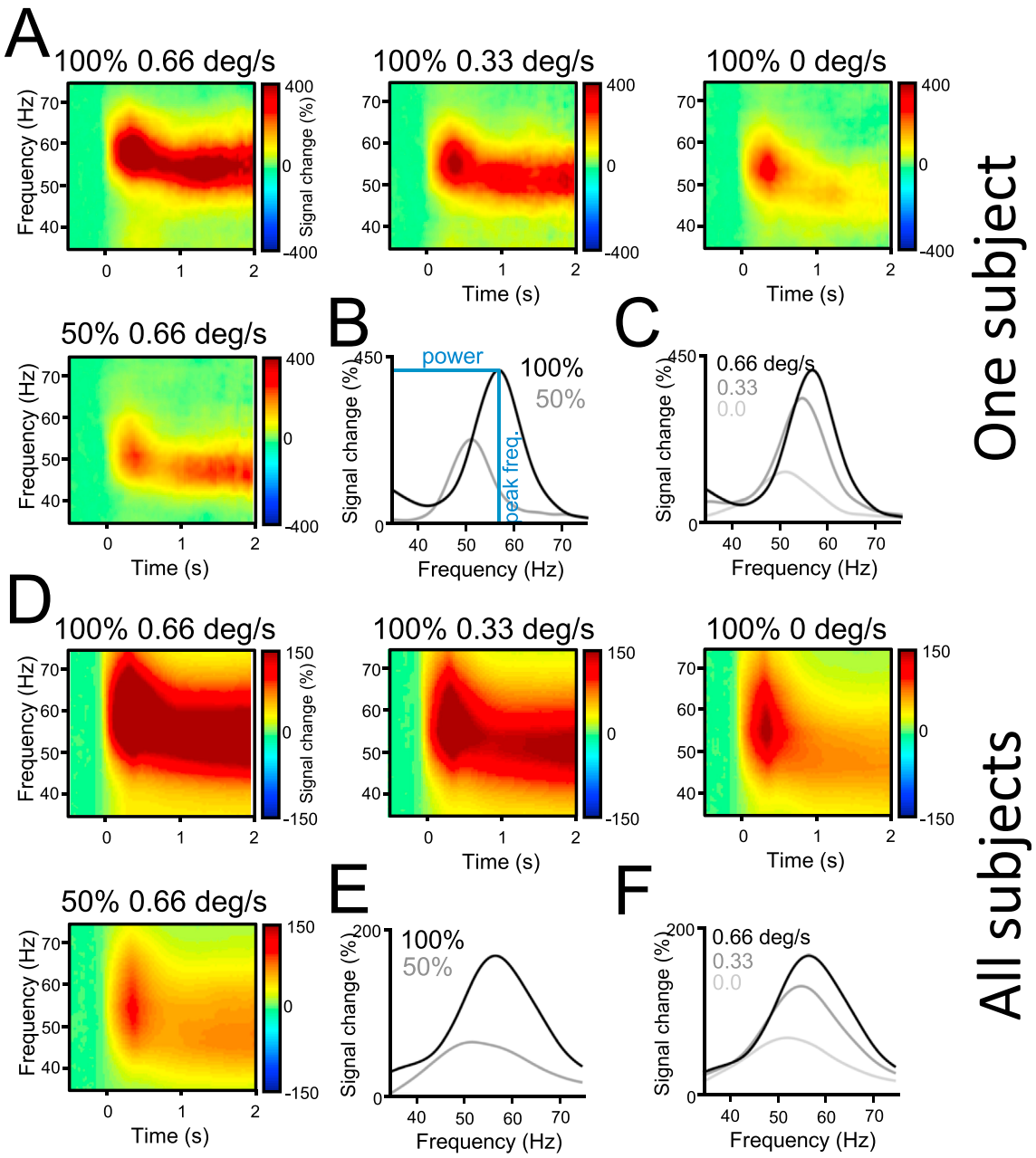

Fig. 2. ***A,*** Time–frequency representations of the gamma–band response in visual cortex of one Example subject to the four different stimulus conditions. Top–left: stimulus with 100% contrast, 0.66 deg/s velocity; top–middle: 100% contrast, 0.33 deg/s velocity; top–right: 100% contrast, 0 deg/s velocity; bottom–left: stimulus with 50% contrast, 0.66 deg/s velocity. ***B,*** Relative increase in spectral power within the gamma–band for the same subject as in ***A*** to the stimuli with 100% contrast, 0.66 deg/s velocity (black), and 50% contrast, 0.66 deg/s velocity (gray) during the sustained activation epoch (0.6s–3.0s after stimulus onset), relative to baseline levels (−1.0 to −0.1s relative to stimulus onset). Blue lines denote gamma peak amplitude and peak frequency estimates. ***C,*** Signal change spectra as in ***B***, but now for the three conditions with different stimulus velocity (all at 100% contrast). ***D-F,*** Group-averages. Spectra are analogous to panels A–C, but now averaged over all 158 subjects.

condition may have been qualitatively different. All conditions were presented equally often (160 trials each), and presented randomly interleaved. Trials were distributed across 16 blocks, with rest periods in between. The experiment lasted approximately 60 min in total. Before the experiment started, subjects performed a small number of practice trials, to become familiar with the task.

Typically within a week after the MEG task, subjects underwent a T1–weighted, structural MRI scan, at either 1.5 or 3.0 T (Siemens, Erlangen, Germany). These anatomical scans were used for MEG source analysis and for quantification of cortical size.

MEG data analysis

All MEG data analyses were performed using Matlab (Mathworks) and the FieldTrip toolbox for electrophysiological data analysis (Oostenveld et al., 2011).

Artifact removal

Trials were defined as the epochs from 1.1 s before stimulus onset until the moment of stimulus velocity increase. Very rarely, subjects

pressed the response button before the velocity increase, and data from these trials were included until the moment of the button press. 50 Hz line noise was removed by applying a discrete Fourier transform (DFT) on the trial data, with data padding to 10 s for optimal filtering (Schoffelen et al., 2011). Subsequently, artifacts were removed based on a semi–automatic routine: EOG data were used to detect putative eye blinks and fixation breaks, and MEG data were used to detect putative muscle artifacts and squid jumps; all putative artifacts were visually inspected and subsequently, data epochs with identified artifacts were removed. Artifact removal was performed blindly with regard to intrinsic or extrinsic factors. On average, 6.1% of all epochs were rejected, and this fraction did not correlate with any of the extrinsic or intrinsic factors under study.

Virtual sensors

Since our stimulus was presented foveally, it activated the visual cortex of both hemispheres. Therefore, two virtual sensors were reconstructed, one in each hemisphere, at the cortical location that fitted best with the observed MEG data within a 40–80 Hz gamma-frequency range in that hemisphere. Per location, the x, y, and z–components were reconstructed separately, leading to a total of six source data time courses per subject. To this end, we used linearly constrained minimum variance (LCMV) spatial filtering (Van Veen et al., 1997). This time–domain beamformer method was used to optimize signal–to–noise ratios, by optimally suppressing non–cortical sources of variance. It also allowed for complete removal of the low–frequency artifacts caused by metallic orthodontic retainers that were worn by 25 subjects in our cohort (Cheyne et al., 2007). To find the two virtual sensor locations, LCMV spatial filters were first computed for a cubic 6 mm–spaced grid of dipole positions, for each subject individually, based on the leadfield matrices at these positions and the data covariance matrix among all MEG channels (van Pelt and Fries, 2013). Data for all conditions were pooled for this computation, leading to common filters for the four experimental conditions. Forty to eighty Hertz bandpassed data from both baseline (−1.0 to −0.1s) and activation (0.6–3.0s) epochs were used as input for the filter estimations. Subsequently, the data were passed through these filters, and interpolated to determine the location with the highest source power levels when comparing activation to baseline. For this specific interpolated location (one in each hemisphere), new spatial filters were computed, and here, the virtual channel time course was reconstructed by multiplying the spatial filter with the sensor–level data. As expected, the gamma–band response localized to early visual cortex in all subjects.

Spectral analysis

First, to investigate the temporal development of the gamma–band response, time and frequency–resolved power analyses were performed at the source–level data for each subject, and for all four stimulation conditions separately. The resulting time–frequency representations (TFRs) were used for quality control by means of visual inspection, to identify potential artifacts in the data. Per subject, TFRs were averaged over the two source locations and their three orientation components. The time window of analysis was −0.7–2.7 s relative to stimulus onset. Sliding windows of 500 ms length were defined in 0.03 s time steps. Data in those windows were multiplied with 3 tapers constituting a discrete prolate spheroidal (Slepian) sequence (Mitra and Pesaran, 1999), to obtain a spectral smoothing of ±4 Hz.

The main spectral analysis involved a fast–Fourier transform (FFT) to determine the peak frequency and maximum amplitude of the gamma–band response induced by each of the four different visual stimulation conditions. FFT analysis was performed for each subject's six virtual sensors (two hemispheres x three orientations), for all four conditions. Baseline–data (−1.1 to −0.1 s before stimulus onset) and sustained activation data (0.6 to maximally 3.0s) were first cut into as many non–overlapping epochs of 500 ms as possible. Data from each of these epochs were multiplied with 3 Slepian tapers, zero padded to 10 s, and Fourier transformed to obtain power estimates between 30 and 90 Hz with a spectral smoothing of ±4 Hz. As with the TFR, the FFT output was averaged over the two source locations and their three orientation components.

Hereafter, a spectrum of the relative change in gamma power was computed by dividing power during visual stimulation by power during the baseline period. Subsequently, per subject and condition, peak frequency and amplitude (expressed as percentage power change from baseline) were quantified. For this, the change spectrum was first smoothed with a Butterworth filter, and subsequently, a second–order polynomial was fitted to the smoothed spectrum. Higher–order polynomials were used for asymmetric spectra. When the peak is determined directly from the raw power change spectrum, then the frequency resolution of the spectrum and noisy fluctuations near the peak have a detrimental effect on the accuracy of the peak frequency estimate. This is overcome by fitting an appropriate mathematical function and determining the peak of that function, because the function smooths over the noisy fluctuations and effectively interpolates and upsamples the data. We found empirically that the polynomial is an excellent fit to the change spectra, and that the fit is further optimized by prior smoothing through a Butterworth filter. We used this procedure previously (van Pelt and Fries, 2013). Fitted spectra were visually inspected by one of the authors (SvP), blind to the stimulus condition, and spectra that did not contain a clear gamma–band peak (ranging from 3 to 12% of the subjects, depending on condition) were not used in further analysis.

MRI dataset

MRI data acquisition, preprocessing, and analysis were performed in the framework of the brain imaging genetics (BIG) study (Franke et al., 2010).

MRI acquisition and processing

MRI data were acquired with either a 1.5–Tesla Siemens Sonata or Avanto scanner or a 3– Tesla Siemens Trio or TimTrio scanner (Siemens Medical Systems, Erlangen, Germany). To obtain a high–resolution structural T1–weighted image, a volumetric magnetization prepared rapid gradient echo (MPRAGE) sequence with a $1.0 \times 1.0 \times 1.0$ mm voxel size was used. Given that images were acquired using different scanners, there was a slight variation in the parameters used. The following repetition time/inversion time/echo time TR/TI/TE/sagittal–slice combinations were applied: 2300/1100/(3.03 or 2.96)/192, 2250/850/(2.95 or 3.68)/176 and 2730/1000/2.95/176.

T1 images were processed using FreeSurfer's (v5.3) default "recon–all'' pipeline (Fischl et al., 2002), which performs automated bias field correction, spatial normalization, skull stripping, and segments brain tissue into cortical gray/white matter, as well as into several non–cortical tissues.

Anatomical parcellation

Cortical segmentation, volumetric estimates, and quality control were performed following the harmonized protocol, developed by the ENIGMA consortium (Thompson et al., 2014) and available at the ENIGMA website (http://enigma.ini.usc.edu/protocols/imaging–protocols/).

Regional cortical volumes were derived from FreeSurfer's cortical anatomical parcellations, according to the Desikan atlas (Desikan et al., 2006). In this atlas, the occipital lobe is represented by the following four bilateral structures: lingual gyrus, pericalcarine cortex, cuneus, and lateral occipital cortex.

Quality control was performed according to the EMIGMA protocol and consisted of visually checking individual images, plotted from both internal (axial and coronal) as well as external (lateral and medial) views.

Individual measurements derived from poorly segmented structures (i.e. where tissue labels were assigned incorrectly), and in some cases, whole images were excluded from subsequent analyses.

Results

Example subject and population distribution

We measured gamma–band responses to inward-moving, concentric visual grating stimuli (Fig. 1) of two contrasts and three velocities in 158 human subjects using MEG. Fig. 2A shows the time–frequency representations (TFRs) of visually induced power changes for a source in visual cortex of an Example subject, separately for each of the four stimulus conditions. Spectra were calculated for frequencies between 30 and 90 Hz, because this range covers the gamma–band for all subjects under the present stimulus conditions, and because source reconstruction was based on this band to avoid the influence of high–power low–frequency rhythms. TFRs of stimulus conditions with different velocities, all at 100% contrast, are displayed horizontally, whereas TFRs for the two different contrasts, both at 0.66 deg/s velocity, are ordered vertically. In all TFRs, it can be seen that GBA increased after stimulus onset (t = 0s), up to 400% relative to pre–stimulus baseline levels. The response was narrow–band, initially at a relatively high frequency, and settled into a slightly lower frequency after around 0.5 s of visual stimulation. The gamma–band response in this subject was strongest for the maximum contrast, maximum velocity condition (upper left). Both amplitude and peak frequency were lower for slower stimulus velocity and for lower stimulus contrast. Fig. 2B shows the spectral power during the sustained activation epoch (0.6–3.0 s) as percent change relative to the pre-stimulus baseline epoch (−1.1 to −0.1 s). The black (gray) line shows this for the stimulus with a velocity of 0.66 deg/s and a contrast of 100% (50%). The blue lines illustrate the derivation of the gamma peak frequency and gamma peak amplitude. These were derived separately for each subject and condition. Fig. 2C shows the corresponding power change spectra for the three velocity conditions presented at 100% contrast.

Fig. 2D–F shows the same analyses averaged over all 158 participants. This confirms the effects of extrinsic factors that we observed in the Example subject. The gamma band appears broader in the average due to gamma-frequency variability across subjects. Average peak frequency (signal change) was 49.9 Hz (68%) for the 50% contrast, 0.66 deg/s velocity condition, 56.2 Hz (184%) for the 100% contrast, 0.66 deg/s velocity condition, 52.4 Hz (141%) for the 100% contrast, 0.33 deg/s velocity condition, and 50.0 Hz (74%) for the 100% contrast, 0.0 deg/s velocity condition. To investigate this variability in relation to intrinsic factors and their interaction with extrinsic factors, the following analyses use the gamma peak frequency and peak amplitude metrics derived per subject as illustrated in Fig. 2B.

Fig. 3 shows the population distribution of gamma peak amplitude and frequency for the 100% contrast, 0.66 deg/s velocity condition, which was the stimulus that yielded the strongest power increase across the entire pool of subjects (see Fig. 2D). The distributions of gamma peak amplitudes (Fig. 3A) did not differ significantly from a lognormal distribution (Lilliefors' test, $p = 0.27$), with a log–mean value of 209% (SD 61.7%) and a maximum of 785%. The distribution of gamma peak frequencies did not differ significantly from a normal distribution (Lilliefors' test, $p = 0.82$), with a mean of 56.2 Hz (SD 5.4) and a range from 41.5 to 72.9 Hz (Fig. 3B). Fig. 3C shows that there was a weak, negative correlation between peak frequency and amplitude ($p < 0.05$).

Extrinsic effects

In the experiment, we aimed at quantifying the effects of extrinsic factors and intrinsic factors on GBA. Fig. 4A shows a scatter plot across subjects of the gamma peak amplitude for the 100% contrast versus 50% contrast stimulus, keeping stimulus velocity constant at 0.66 deg/s. Amplitudes were highly correlated between contrast conditions, across subjects ($r = 0.84$, $p < 0.001$), suggesting that a substantial part of amplitude variability was subject specific, that is, dependent on intrinsic factors as investigated further below. In addition, there was a clear effect of the extrinsic factor stimulus contrast: amplitudes increased with stimulus contrast for each individual subject, leading to a 2.2–fold increase in average gamma amplitude (paired t–test, $p < 0.001$). Gamma power change values were on average 106% (SD 84%) in the 50% contrast condition, and 247% (SD 168%) in the 100% contrast condition. Given that a previous study reported that gamma–band power induced in human visual cortex by grating stimuli is linearly dependent on stimulus contrast (Hadjipapas et al., 2015), we also performed a linear fit between gamma power change and stimulus contrast. This revealed a 2.8% absolute increase in gamma power for each 1% absolute increase in stimulus contrast (Fig. 4B).

Next, we investigated gamma peak frequency (Fig. 4C). Peak frequencies were also highly correlated between the two conditions, across subjects ($r = 0.78$, $p < 0.001$), again suggesting a substantial intrinsic component. Frequencies were higher for the 100% contrast than for the 50% contrast stimulus ($p < 0.001$). Interestingly, this difference between contrast conditions shrunk for higher gamma peak frequencies, suggesting a ceiling effect. This is supported by the fact that the regression line, shown in red, approached the diagonal for higher frequencies. To further illustrate this, Fig. 4E shows the ratio of the peak frequencies at 100% and 50% as a function of the peak frequency at 50%, computed as a

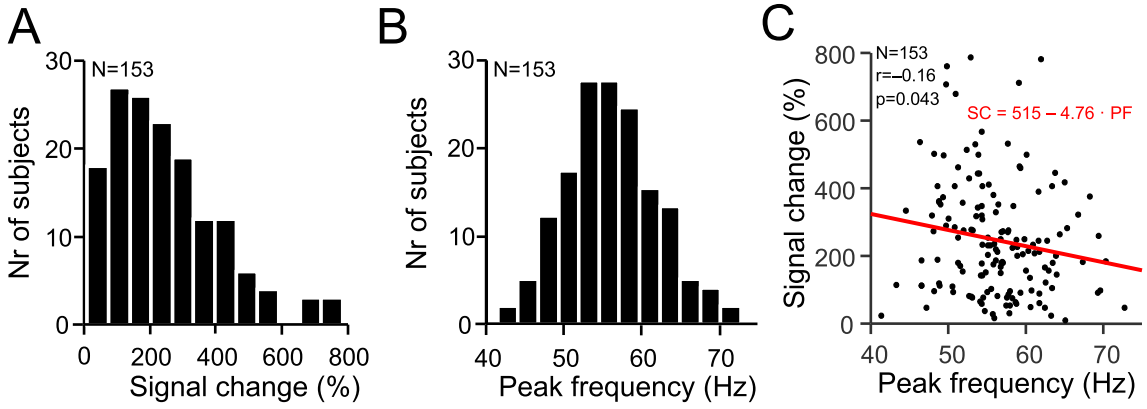

Fig. 3. Population distributions. ***A,*** Histogram of gamma peak amplitudes across the population of subjects for the stimulus with 100% contrast and 0.66 deg/s velocity. ***B,*** Same as ***A***, but for gamma peak frequencies. ***C,*** Correlation between peak frequency and power increase for the same stimulus. Each data point represents one subject.

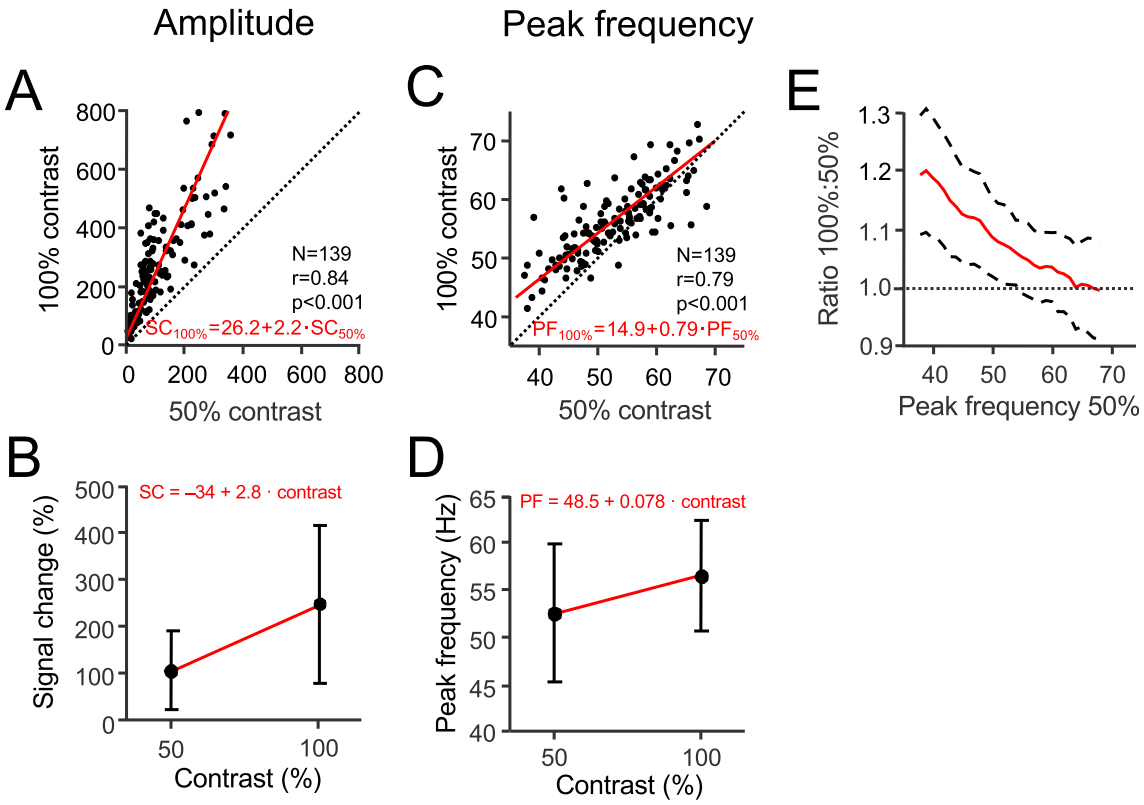

Fig. 4. Effect of stimulus contrast on gamma–band activity. ***A,*** Gamma peak amplitudes for a 100% contrast stimulus (y–axis) versus a 50% contrast stimulus (x–axis). Each data point denotes a single subject. The linear regression is shown in red. ***B,*** Gamma peak amplitude, averaged across the population (±SD) as function of stimulus contrast. ***C,*** Gamma peak frequency for a 100% contrast stimulus (y–axis) versus a 50% contrast stimulus (x–axis). ***D,*** Gamma peak frequency, averaged across the population (±SD) as function of stimulus contrast. ***E,*** Ratio between gamma peak frequencies for a 100% and a 50% contrast stimulus, as a function of the gamma peak frequencies for the 50% contrast stimulus. The red line shows the moving average of this ratio (averaging window of 9 Hz). Dashed lines show the average ± 1 SD.

moving average over the frequency range (dashed lines indicate mean ± 1 SD). This analysis revealed that the higher a subject's gamma–band peak frequency was in response to the 50% contrast stimulus, the less this peak frequency increased for the 100% stimulus. The effect of contrast, to increase peak frequency, vanished, but did not reverse, at the upper end of the gamma band. Fig. 3D reports the gamma peak frequency values for both contrast conditions: Gamma peak frequency was on average 52.4 Hz (SD 7.3 Hz) for 50% contrast, and 56.3 Hz (SD 5.8 Hz) for 100% contrast. Also for gamma peak frequency, a previous study reported a linear dependence on stimulus contrast (Hadjipapas et al., 2015), and we therefore performed a linear fit. This revealed that gamma peak frequency increased by 0.078 Hz per 1% absolute increase in stimulus contrast.

The effect of stimulus velocity on amplitude and peak frequency is summarized in Fig. 5 in an analogous fashion to Fig. 4. Similar to stimulus contrast, stimulus velocity also increased both gamma peak amplitude and frequency. Fig. 5A and B shows that for the large majority of subjects, higher stimulus velocities induced larger gamma peak amplitudes. This held both, for the comparison between stationary and slowly moving (0.33 deg/s) stimuli (Fig. 5A; paired *t*-test $p < 0.001$), and for the comparison between the two stimulus velocities (0.33 deg/s versus 0.66 deg/s) (Fig. 5B; $p < 0.001$). Average gamma amplitudes increased approximately linearly with the employed stimulus velocities (Fig. 5C), with a 216% absolute increase per 1 deg/s increase in stimulus velocity. Fig. 5D and E shows that stimulus velocity affected also gamma peak frequency. This again held both for the comparison between stationary and slowly moving stimuli (Fig. 5D, $p < 0.001$) and for the comparison between the two stimulus velocities (Fig. 5E, $p < 0.001$). Fig. 4G and H shows the ratio between peak frequencies as a function of the peak frequency in the lower velocity condition. This revealed a similar frequency ceiling effect as observed for the comparison between different contrast conditions. Fig. 5F shows that the average gamma peak frequency increased approximately linearly with stimulus velocity, with a 7.2 Hz frequency increase per 1 deg/s stimulus velocity increase.

Intrinsic effects

We next investigated the dependence of gamma peak amplitude and frequency on intrinsic, subject–specific factors, in particular age, sex and cortical volumetrics. These analyses used gamma–band responses obtained with stimuli of 100% contrast and 0.66 deg/s velocity. We derived subject-wise gamma peak frequencies and amplitudes for this single stimulus condition, rather than averaging over all conditions, because 1) gamma with this stimulus exhibited the highest signal-to-noise ratio, and 2) averaging over stimulus conditions could in some cases render gamma peaks highly asymmetric or even double peaked.

We first investigated the relation between gamma–band parameters and occipital cortical volumetrics (Fig. 6). The subjects' T1–weighted MRI scans were used together with the Desikan–Killiany atlas (Desikan et al., 2006) to define in each subject the occipital cortex and to derive from it the following volumetric parameters: cortical thickness, surface area and volume (see Methods). We found no consistent relationship between gamma peak amplitude and cortical thickness, area or volume (Fig. 6A–C; $p > 0.1$ in all cases). By contrast, gamma peak frequency was correlated with thickness and area, and not with volume. Thickness correlated positively with peak frequency (Fig. 6D; $r = 0.25$, $p < 0.01$), with a 13.4 Hz increase per mm increase in gray matter thickness. Area correlated negatively with peak frequency (Fig. 6E; $r = -0.18$, $p < 0.05$), with a decrease of 0.044 Hz per cm^2 increase in area. Finally, cortical volume did not systematically relate to peak frequency (Fig. 6F; $p > 0.1$).

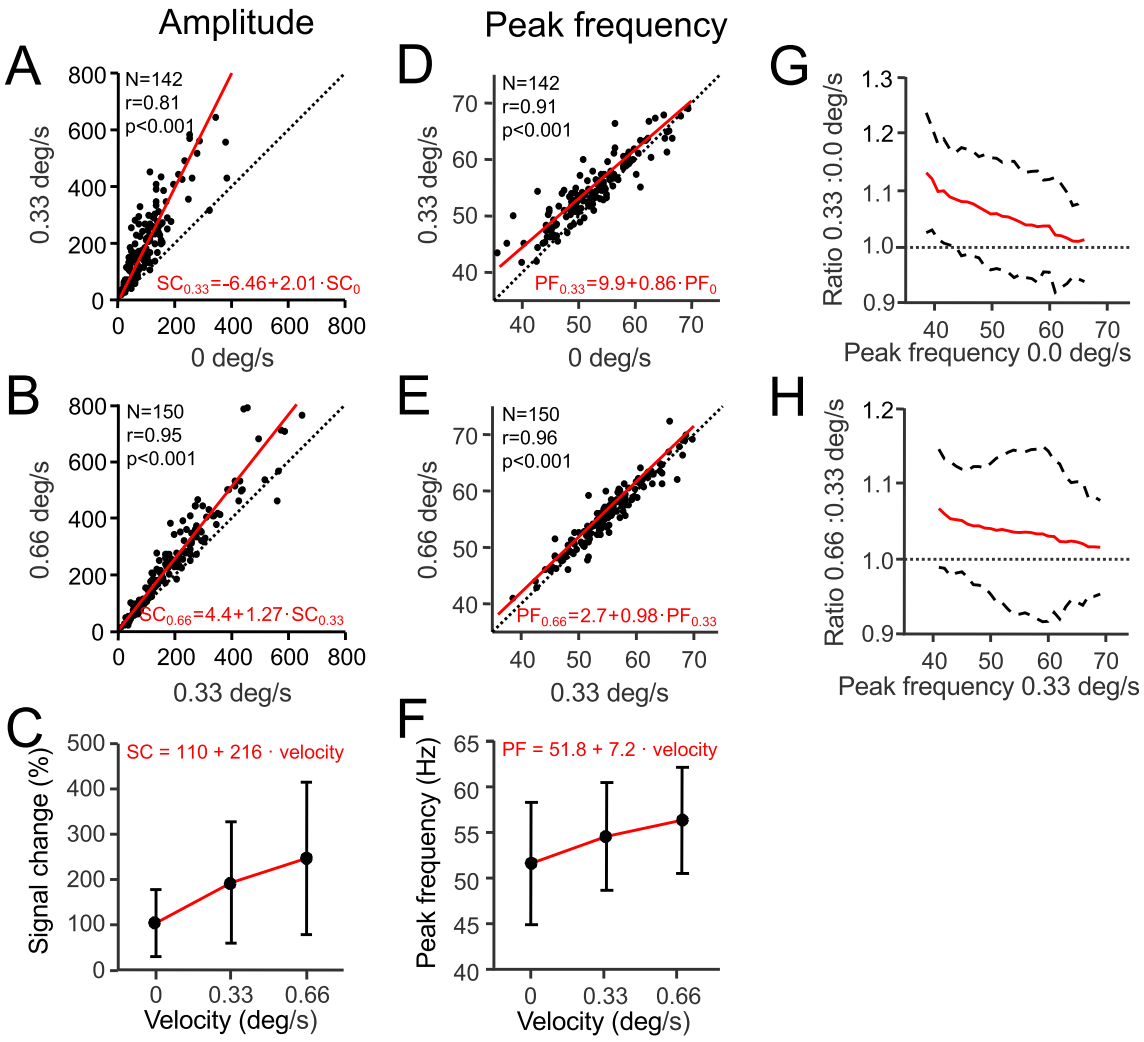

Fig. 5. Effect of stimulus velocity on gamma–band activity. ***A,*** Gamma peak amplitudes for a 0.33 deg/s stimulus (y–axis) versus a static stimulus (x–axis). Each data point denotes a single subject. The linear regression is shown in red. ***B,*** Same as in ***A***, but comparing a 0.66 deg/s stimulus (y–axis) with a 0.33 deg/s stimulus (x–axis). ***C,*** Gamma peak amplitude, averaged across the population (±SD) as function of stimulus velocity. ***D.*** Gamma peak frequency for a 0.33 deg/s stimulus (y–axis) as function of gamma peak frequency for a static stimulus (x–axis). ***E.*** Gamma peak frequency for a 0.66 deg/s stimulus (y–axis) as function of gamma peak frequency for a 0.33 deg/s stimulus (x–axis). ***F,*** Gamma peak frequency, averaged across the population (±SD) as function of stimulus velocity. ***G,*** Ratio between gamma peak frequencies for a 0.33 deg/s and a static stimulus, as a function of the gamma peak frequencies for the static stimulus. The red line shows the moving average of this ratio (averaging window of 9 Hz). Dashed lines show the average ± 1 SD. ***H,*** Ratio between gamma peak frequencies for a 0.66 deg/s and a static stimulus, as a function of the gamma peak frequencies for the 0.33 deg/s stimulus.

In a further analysis, we subdivided occipital cortex into pericalcarine cortex, containing primary visual cortex, and the remaining occipital region, which we refer to as extra–pericalcarine. Tables 1 and 2 show the resulting correlation analyses for these regions separately. For amplitude, this approach confirmed the absence of any effect. For peak frequency, it revealed that the correlation with cortical thickness was driven by the extra–pericalcarine region, whereas the relation with surface area was driven by the pericalcarine region. Interestingly, pericalcarine volume was also found to be negatively correlated with peak frequency, with a decrease of 1.88 Hz per cm^3 increase in volume.

Next, we investigated the effects of age on gamma peak amplitude and peak frequency (Fig. 7). Whereas gamma amplitude showed no significant relationship with age (Fig. 7A; $p = 0.33$), peak frequency decreased significantly with age, with a rate of −0.52 Hz/year (Fig. 7B; $r = -0.33$, $p < 0.001$). Notably, of the anatomical measures discussed in Fig. 5, also cortical thickness correlated negatively with age (Fig. 7C; $r = -0.30$, $p < 0.01$), while gray matter area and volume did not show a significant correlation (data not shown, $p > 0.05$ in both cases). This suggests that the effect of age might be due to the decrease in cortical thickness over age. We tested this by performing a multiple linear regression analysis that included both predicting factors (age and cortical thickness). This revealed that both factors contributed significantly to the correlation with gamma peak frequency ($p < 0.01$, $p < 0.05$, respectively). That is, both age and cortical thickness likely had independent effects on gamma peak frequency.

Finally, we looked at sex differences (Fig. 8). This revealed that gamma amplitude was not different between the two sexes (Fig. 8A; $p = 0.71$, independent two-sample t–test). In contrast, gamma peak frequency was higher for women (mean 57.0 Hz, SD 5.9 Hz) than for men (mean 54.9, SD 5.4 Hz) (Fig. 8B; $p < 0.05$, Student t–test). This sex effect persisted when taking into account the distributions in age and cortical thickness of the two sex groups ($p < 0.05$, multiple linear regression with the independent variables age, cortical thickness and sex; sex was coded as a 1 for males and as a 2 for females). The effect could also not be explained by differences in 1/f shape. If women had a stronger 1/f dropoff in the power spectrum, the percent change spectrum might appear to be shifted to higher frequencies. To test for this, we fitted a power-law function to each subject's gamma spectrum. The resulting

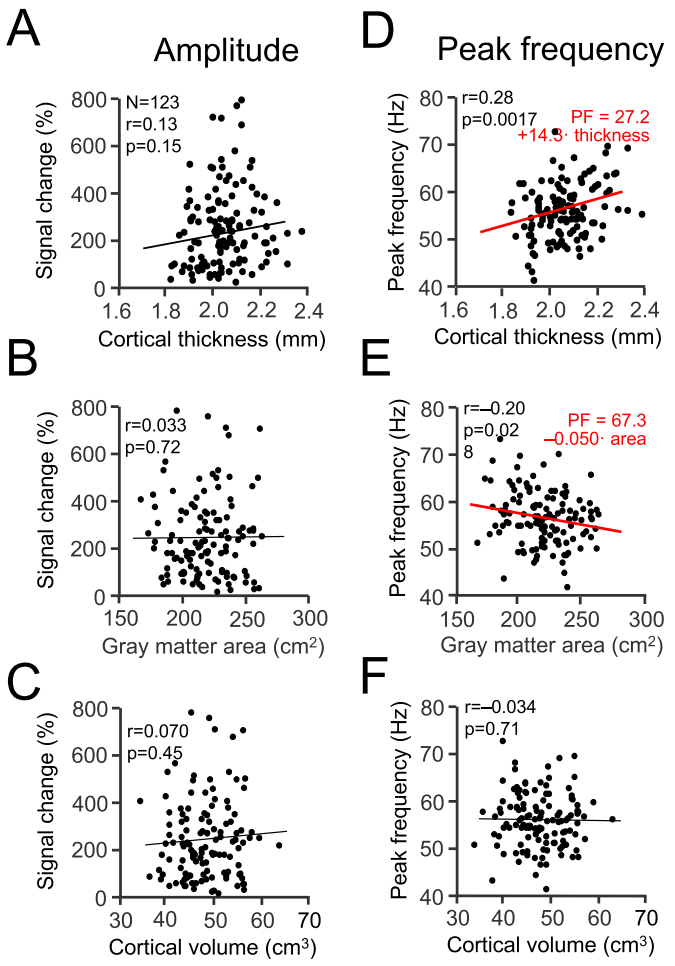

Fig. 6. Relation between gamma–band activity as induced by the stimulus with 100% contrast, 0.66 deg/s velocity, and cortical volumetrics. ***A,*** Gamma peak amplitudes as a function of the thickness of occipital cortex, i.e. the combination of bilateral pericalcarine, cuneus, lingual, and lateral occipital regions. The black line shows the regression line of the (non–significant) correlation between these parameters. ***B,*** Gamma peak amplitudes as a function of total gray matter area within the occipital cortex. ***C,*** Gamma peak amplitudes as a function of total gray matter volume within the occipital cortex. ***D-F,*** Same as ***A-C***, but for gamma peak frequency.

Table 1
Statistics of the relation between gamma peak amplitudes and thickness, area, and volume of the bilateral pericalcarine regions (left–hand columns), and that of the bilateral non–pericalcarine occipital regions (right–hand columns). N = 123.

Amplitude	Pericalcarine			Other occipital		
	r	p	β	r	p	β
Thickness	0.11	0.21	–	0.13	0.15	–
Area	0.066	0.47	–	0.030	0.74	–
Volume	0.093	0.31	–	0.063	0.49	–

regression coefficients were not significantly different between males and females (p = 0.32; independent *t*-test).

Combined effects

In order to estimate the total variance in gamma peak amplitude and frequency that is explained by intrinsic and extrinsic factors, we performed a multiple linear regression with the independent factors stimulus contrast, stimulus velocity, subject sex, and subject age (Fig. 9). Cortical volumetric parameters were not included as factors, because of their high covariation with age (Fig. 7C). Fig. 9A shows that a weighted combination of these four variables explained 20% of the observed variance in gamma–band amplitude across the conditions and subjects (r = 0.45, p < 0.001). Similarly, a differently weighted combination of the same factors explained 21% of the observed variance in gamma peak frequency (Fig. 9B; r = 0.46, p < 0.001). Lastly, we performed a canonical correlation between gamma amplitude and peak frequency on the one hand, and stimulus contrast, stimulus velocity, subject sex, and subject age on the other (Figs. 8, 9). For a given set of variables, a canonical correlation analysis will identify the linear combination between them that has the maximum correlation. The analysis revealed that contrast, velocity, sex, and age could explain a maximum of 31% of the observed variance in a weighted combination of gamma–band amplitude and peak frequency (r = 0.56, p < 0.001).

Table 2
Statistics of the relation between gamma peak frequencies and thickness, area, and volume of the bilateral pericalcarine regions (left–hand columns), and that of the bilateral non–pericalcarine occipital regions (right–hand columns). For significant correlations (p < 0.05; in red), the slope β of the regression is provided. N = 123.

Peak Frequency	Pericalcarine			Other occipital		
	r	p	β	r	p	β
Thickness	0.023	0.80	–	0.28	0.0016	13.7
Area	−0.33	<0.001	−0.42	−0.16	0.084	–
Volume	−0.26	0.0042	−1.88	0.0067	0.94	–

Discussion

We quantified gamma peak amplitude and peak frequency in a large cohort of healthy subjects. Across the sample of subjects, gamma peak frequencies were distributed normally, and visually induced gamma power changes were distributed log–normally. Gamma power changes and gamma peak frequencies were weakly correlated with each other. The extrinsic factors stimulus contrast and stimulus velocity correlated positively with both gamma–band parameters, with peak frequencies showing a ceiling effect. Also several intrinsic, subject-specific factors affected gamma parameters. Peak frequency increased with average cortical thickness within the occipital cortex, decreased with gray matter area, and was not modulated by volume, while gamma amplitude was not modulated by cortical volumetrics. The correlation of peak frequency with thickness was driven by the extra-calcarine region, whereas its correlation with surface area was driven by the pericalcarine region. Increasing age of subjects led to decreases in both cortical thickness and gamma peak frequency. The changes in peak frequency were not fully explained by changes in thickness, because age and thickness had independent effects on peak frequency. Gamma amplitude was not modulated by either age or thickness. Female subjects had a higher peak frequency than male subjects, and this was not due to differences in age or cortical thickness. Gamma amplitudes did not differ between the sexes. Extrinsic and intrinsic factors together explained approximately 20% of both peak frequency and amplitude, and 30% of an optimally weighted combination of both.

Note that the tests involving gamma amplitude and peak frequency cannot be compared directly, because amplitude estimates are affected by the distance between sources and sensors, whereas peak frequency estimates are immune to this. We used source analysis to minimize effects of head position in the MEG helmet. However, this cannot fully eliminate these effects. Correspondingly, previous studies have reported that gamma amplitude has a lower test–retest reliability than peak frequency (Muthukumaraswamy et al., 2010), and is also less heritable than peak frequency (van Pelt et al., 2012). Note also that amplitude estimates can be affected by the $1/f^n$ background in MEG signal power. In any case, our analyses likely had a lower sensitivity for amplitude than frequency effects, which might underlie some of our negative findings on the relation

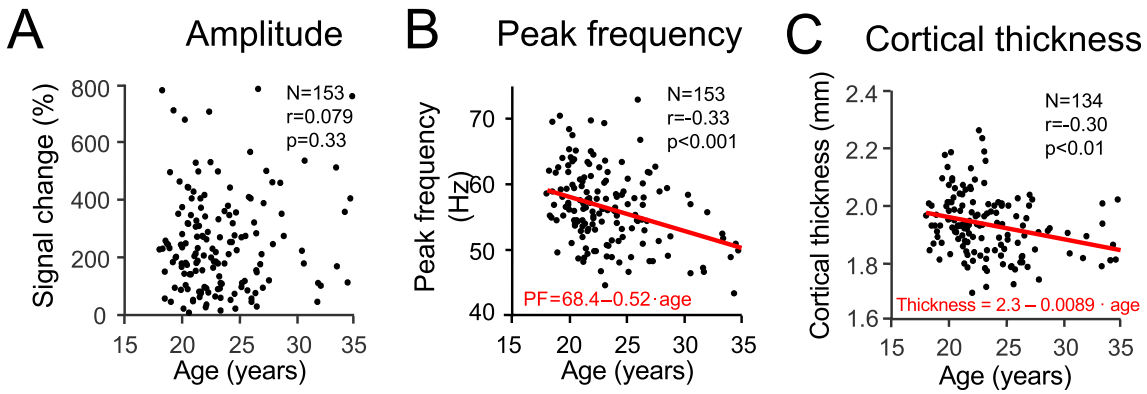

Fig. 7. Effects of age. ***A,*** Gamma peak amplitudes as a function of age, for the stimulus with 100% contrast, 0.66 deg/s velocity. ***B,*** Gamma peak frequencies as a function of age, for the same stimulus. The red regression line denotes the significant relation between the two parameters. ***C,*** Cortical thickness averaged over bilateral pericalcarine, cuneus, lingual, and lateral occipital regions, as function of age. The red regression line denotes the significant relation between the two parameters.

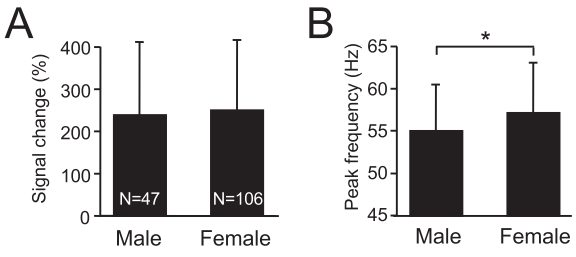

Fig. 8. Sex differences. ***A***, Average gamma peak amplitude for male and female subjects, for the stimulus with 100% contrast, 0.66 deg/s velocity. Error bars denote 1 SD. ***B,*** Average gamma peak frequency for male and female subjects.

between amplitude and intrinsic factors.

This study, for the first time, characterizes the cross–subject distributions of gamma amplitudes and peak frequencies as lognormal and normal, respectively (Fig. 3A and B), which was aided by the large sample size. Amplitude and peak frequency are negatively correlated (Fig. 3C), yet we cannot rule out that this is at least partly due to the above–mentioned interaction between amplitude estimation and $1/f^n$ background power. Previous studies testing for an amplitude-frequency relation have not found it, even when using relatively large sample sizes (e.g. Robson et al., 2015; Swettenham et al., 2009). Our observed peak frequency range of 40–75 Hz corresponds with values found in other human visual gamma studies using similar stimuli (van Pelt et al., 2012; Muthukumarashwamy et al., 2010; Cousijn et al., 2014; Hadjipapas et al., 2015). The considerable variability in amplitude values also corresponds to that reported in previous work. Note that comparisons of amplitude values between studies are problematic for the reasons mentioned above.

In the following, we will first compare the effects of extrinsic and intrinsic factors observed here with previous studies, and subsequently discuss the possible underlying mechanisms. The effects of extrinsic factors on gamma are qualitatively and quantitatively similar to those reported in previous studies. The increase of both gamma amplitude and peak frequency with increasing stimulus contrast (Fig. 4) confirms the effects found before in both human and monkey experiments (Ray and Maunsell, 2010; Roberts et al., 2013; Jia et al., 2013; Hadjipapas et al., 2015). Also stimulus velocity (Fig. 5) has been known to modulate gamma power and frequency (Swettenham et al., 2009; Stroganova et al., 2015; Orekhova et al., 2015). In contrast to our findings, Swettenham et al. (2009) did not find significant increases in gamma amplitude, which might be explained by differences in sample size. Interestingly, they reported a similar saturation effect of the peak frequency increase for higher frequencies (Fig. 5E).

The effects of intrinsic factors concur partly with previous studies. Increasing age led to a decline in gamma frequency, in agreement with previous studies (Gaetz et al., 2012; Robson et al., 2015). We also investigated the relation between cortical thickness and gamma for

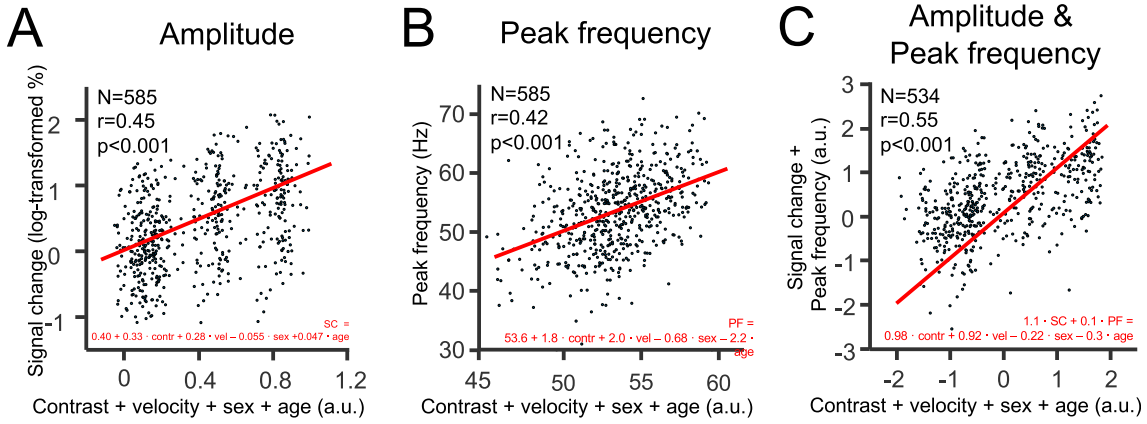

Fig. 9. Combined effects of extrinsic and intrinsic factors. ***A,*** Correlation between gamma peak amplitudes and stimulus contrast, stimulus velocity, sex and age. Data for all four stimulus conditions are included in this analysis, leading to a maximum of four data points per subject. The red line denotes the regression line of the correlation. ***B,*** Correlation between gamma peak frequencies and stimulus contrast, stimulus velocity, sex and age. ***C,*** Canonical correlation between gamma peak amplitudes and peak frequencies with stimulus contrast, stimulus velocity, sex and age.

several different cortical regions. The pericalcarine region corresponds to primary visual cortex, which is a particularly strong source of visual gamma. For this region, we found no relation between cortical thickness and gamma, in agreement with previous studies (Perry et al., 2013; Schwarzkopf et al., 2012; Robson et al., 2015). However, when we extended the analysis beyond the pericalcarine region, we found a positive relation between gamma frequency and cortical thickness, which has not been reported so far. We also investigated the relation between gamma and brain region surface area. Several previous studies reported an increase in gamma frequency with the surface area of areas V1 or V2 (Gregory et al., 2016; Schwarzkopf et al., 2012; Perry et al., 2013). By contrast, we find a negative correlation between surface area and gamma peak frequency. This effect is significant, when several occipital areas are combined, and it is mainly driven by the pericalcarine region. This negative relation between surface area and gamma frequency in the pericalcarine might also drive the observed negative relation between cortical volume and gamma frequency, which we observed only in the pericalcarine. Previous studies that tested for such a relation did not reveal it, possibly due to smaller sample size (Gaetz et al., 2012; Perry et al., 2013). Finally, we report for the first time that women have on average a higher gamma peak frequency than men.

Mechanisms

Gamma activity arises from interactions in networks of mutually connected excitatory and inhibitory neurons (Whittington et al., 2000; Tiesinga and Sejnowski, 2009). Within the gamma cycle, excitatory neurons activate inhibitory neurons, which in turn inhibit both the excitatory neurons and themselves. When inhibition declines according to its characteristic time constant, excitation surpasses it and thereby starts the next gamma cycle.

The main effects of extrinsic factors are an increase in gamma amplitude and peak frequency for stimuli of higher contrast or higher velocity. Higher contrast corresponds to stronger excitatory drive, and this likely makes excitation overtake inhibition earlier in the gamma cycle and thereby to increase gamma frequency. Higher velocity might for some neurons also correspond to stronger excitatory drive, yet more generally, it leads to higher stimulus salience. Thereby, the higher gamma peak frequency observed for higher–velocity stimuli might be related to the same effect observed for attended stimuli (Bosman et al., 2012; Fries, 2015). This effect of stimulus salience on gamma frequency might not be simply mediated through stronger excitatory drive. Rather, it might involve inhibitory circuits activated by attention and generally by top–down input (Vinck et al., 2013; Zhang et al., 2014).

Besides the dynamic levels of excitation and inhibition, more structural factors also influence gamma frequency, such as e.g. axonal and synaptic conduction delays, with longer delays resulting in lower frequency. Differences in conduction delays between subjects are a plausible cause of inter–subject differences in gamma peak frequency. We found gamma frequency to be lower for subjects with larger early visual cortex surface area. If the brain area is larger, this might entail that a given visual stimulus activates a larger cortical patch. This larger patch contains neurons at larger distances and thereby coupled through longer-range lateral connections, with correspondingly longer conduction delays, leading to lower gamma peak frequencies. Similar effects have been described, when the size of the activated patch of cortex is varied by varying stimulus size. Stimuli of larger size activate larger cortical patches and induce gamma with lower peak frequency (Gieselmann and Thiele, 2008).

For two observations, namely the higher gamma frequency for subjects with thicker cortex and for female subjects, we currently have no mechanistic explanation. We note that several previous studies have reported a positive correlation between gamma peak frequency and GABA concentration measured via magnetic resonance spectroscopy (MRS) (Muthukumurashwamy et al., 2009; Robson et al., 2015). MRS uses relatively large voxels, including both white and gray matter. We found that thicker gray matter correlates with higher gamma frequency. For subjects with thicker gray matter, the MRS voxel might contain relatively more gray than white matter. Thereby, the correlation of gamma frequency with GABA might in fact be due to a correlation with gray matter thickness. These considerations are also relevant for the effect of age, because age leads to a reduced cortical thickness, reduced GABA in MRS and reduced gamma peak frequency.

Conclusions and outlook

To summarize, both extrinsic and intrinsic factors substantially affect gamma–band activity, with quantitatively comparable effect sizes. Both sources of variability are important to consider when designing and interpreting experiments that investigate gamma–band activity. The current findings, in combination with existing computational models, provide a starting point to further elucidate how local network and genetic properties are involved in generating gamma–band activity in humans and account for its variability. Our results can also aid in further understanding the mechanisms of gamma–related disorders. Both schizophrenia and Autism Spectrum Disorders (ASD) have been associated with reduced gamma-band activity (Peiker et al., 2015; Uhlhaas and Singer, 2006). Also Alzheimer's disease has been related to reduced gamma-band activity, with the additional intriguing finding, that gamma-frequency entrainment through optogenetic stimulation or visual flicker can reduce the concentration of Alzheimer's related proteins (Iaccarino et al., 2016). Thus, gamma is a potential biomarker for those diseases, and the present results suggest that the relevant information in the gamma-band response can best be used in combination with information about age, sex and cortical volumetrics, and by using stimuli that are strictly standardized.

Significance statement

Activated visual cortex engages in gamma-band activity (GBA), which subserves several cognitive functions, including perceptual binding and attention. GBA is influenced by both, extrinsic factors, like stimuli and task, and intrinsic, subject-specific factors, like the subject's genetic makeup. We measured visual GBA in 158 human subjects. In addition to replicating several known extrinsic and intrinsic influences in this unusually large cohort, we report that gamma frequency is higher for thicker and lower for larger visual cortex, and it is higher in female than male subjects. The precise dependence of gamma on extrinsic and intrinsic factors helps understanding the mechanisms underlying the generation of gamma, and the way, in which gamma subserves the cognitive functioning of an individual subject.

Acknowledgements

PF acknowledges grant support by DFG (SPP 1665, FOR 1847, FR2557/5-1-CORNET, FR2557/6-1-NeuroTMR), EU (HEALTH-F2-2008-200728-BrainSynch, FP7-604102-HBP, FP7-600730-Magnetrodes), a European Young Investigator Award, NIH (1U54MH091657-WU-Minn-Consortium-HCP), and LOEWE (NeFF).

References

Adjamian, P., Holliday, I.E., Barnes, G.R., Hillebrand, A., Hadjipapas, A., Singh, K.D., 2004. Induced visual illusions and gamma oscillations in human primary visual cortex. Eur. J. Neurosci. 20, 587–592.

Bosman, C.A., Schoffelen, J.M., Brunet, N., Oostenveld, R., Bastos, A.M., Womelsdorf, T., Rubehn, B., Stieglitz, T., De Weerd, P., Fries, P., 2012. Attentional stimulus selection through selective synchronization between monkey visual areas. Neuron 75, 875–888.

Buzsáki, G., Wang, X.J., 2012. Mechanisms of gamma oscillations. Annu. Rev. Neurosci. 35, 203–225.

Cousijn, H., Haegens, S., Wallis, G., Near, J., Stokes, M.G., Harrison, P.J., Nobre, A.C., 2014. Resting GABA and glutamate concentrations do not predict visual gamma frequency or amplitude. Proc. Natl. Acad. Sci. U.S.A. 111, 9301–9306.

Desikan, R.S., Ségonne, F., Fischl, B., Quinn, B.T., Dickerson, B.C., Blacker, D., Buckner, R.L., Dale, A.M., Maguire, R.P., Hyman, B.T., Albert, M.S., Killiany, R.J.,

2006. An automated labeling system for subdividing the human cerebral cortex on MRI scans into gyral based regions of interest. Neuroimage 31, 968–980.
Fell, J., Klaver, P., Lehnertz, K., Grunwald, T., Schaller, C., Elger, C.E., Fernández, G., 2001. Human memory formation is accompanied by rhinal–hippocampal coupling and decoupling. Nat. Neurosci. 4, 1259–1264.
Fischl, B., Salat, D.H., Busa, E., Albert, M., Dieterich, M., Haselgrove, C., van der Kouwe, A., Killiany, R., Kennedy, D., Klaveness, S., Montillo, A., Makris, N., Rosen, B., Dale, A.M., 2002. Whole brain segmentation: automated labeling of neuroanatomical structures in the human brain. Neuron 33, 341–355.
Franke, B., Vasquez, A.A., Veltman, J.A., Brunner, H.G., Rijpkema, M., Fernández, G., 2010. Genetic variation in CACNA1C, a gene associated with bipolar disorder, influences brainstem rather than gray matter volume in healthy individuals. Biol. Psychiatr. 68, 586–588.
Fries, P., 2015. Rhythms for cognition: communication through coherence. Neuron 88, 220–235.
Fries, P., Reynolds, J.H., Rorie, A.E., Desimone, R., 2001. Modulation of oscillatory neuronal synchronization by selective visual attention. Science 291, 1560–1563.
Fries, P., Schröder, J.H., Roelfsema, P.R., Singer, W., Engel, A.K., 2002. Oscillatory neuronal synchronization in primary visual cortex as a correlate of stimulus selection. J. Neurosci. 22, 3739–3754.
Gaetz, W., Roberts, T.P.L., Singh, K.D., Muthukumaraswamy, S.D., 2012. Functional and structural correlates of the aging brain: relating visual cortex (V1) gamma band responses to age–related structural change. Hum. Brain Mapp. 33, 2035–2046.
Gieselmann, M.A., Thiele, A., 2008. Comparison of spatial integration and surround suppression characteristics in spiking activity and the local field potential in macaque V1. Eur. J. Neurosci. 28, 447–459.
Gregory, S., Fusca, M., Rees, G., Schwarzkopf, D.S., Barnes, G., 2016. Gamma frequency and the spatial tuning of primary visual cortex. PLoS One 11, e0157374.
Hadjipapas, A., Lowet, E., Roberts, M.J., Peter, A., De Weerd, P., 2015. Parametric variation of gamma frequency and power with luminance contrast: a comparative study of human MEG and monkey LFP and spike responses. Neuroimage 112, 327–340.
Hoogenboom, N., Schoffelen, J.M., Oostenveld, R., Parkes, L.M., Fries, P., 2006. Localizing human visual gamma–band activity in frequency, time and space. Neuroimage 29, 764–773.
Hoogenboom, N., Schoffelen, J.M., Oostenveld, R., Fries, P., 2010. Visually induced gamma-band activity predicts speed of change detection in humans. Neuroimage 51, 1162–1167.
Howard, M.W., Rizzuto, D.S., Caplan, J.B., Madsen, J.R., Lisman, J., Aschenbrenner–Scheibe, R., Schulze–Bonhage, A., Kahana, M.J., 2003. Gamma oscillations correlate with working memory load in humans. Cerebr. Cortex 13, 1369–1374.
Iaccarino, H.F., Singer, A.C., Martorell, A.J., Rudenko, A., Gao, F., Gillingham, T.Z., Mathys, H., Seo, J., Kritskiy, O., Abdurrob, F., Adaikkan, C., Canter, R.G., Rueda, R., Brown, E.N., Boyden, E.S., Tsai, L.H., 2016. Gamma frequency entrainment attenuates amyloid load and modifies microglia. Nature 540, 230–235.
Jia, X., Xing, D., Kohn, A., 2013. No consistent relationship between gamma power and peak frequency in macaque primary visual cortex. J. Neurosci. 33, 17–25.
Kujala, J., Jung, J., Bouvard, S., Lecaignard, F., Lothe, A., Bouet, R., Ciumas, C., Ryvlin, P., Jerbi, K., 2015. Gamma oscillations in V1 are correlated with GABA(A) receptor density: a multi–modal MEG and Flumazenil–PET study. Sci. Rep. 5, 16347.
Landau, A.N., Schreyer, H.M., van Pelt, S., Fries, P., 2015. Distributed attention is implemented through theta–rhythmic gamma modulation. Curr. Biol. 25, 2332–2337.
Michalareas, G., Vezoli, J., van Pelt, S., Schoffelen, J.M., Kennedy, H., Fries, P., 2016. Alpha–beta and gamma rhythms subserve feedback and feedforward influences among human visual cortical areas. Neuron 89, 384–397.
Mitra, P.P., Pesaran, B., 1999. Analysis of dynamic brain imaging data. Biophys. J. 76, 691–708.
Muthukumaraswamy, S.D., Edden, R.A., Jones, D.K., Swettenham, J.B., Singh, K.D., 2009. Resting GABA concentration predicts peak gamma frequency and fMRI amplitude in response to visual stimulation in humans. Proc. Natl. Acad. Sci. U.S.A. 106, 8356–8361.
Muthukumaraswamy, S.D., Singh, K.D., Swettenham, J.B., Jones, D.K., 2010. Visual gamma oscillations and evoked responses: variability, repeatability and structural MRI correlates. Neuroimage 49, 3349–3357.
Oostenveld, R., Fries, P., Maris, E., Schoffelen, J.M., 2011. FieldTrip: open source software for advanced analysis of MEG, EEG, and invasive electrophysiological data. Comput. Intell. Neurosci. 2011, 156869.
Orekhova, E.V., Butorina, A.V., Sysoeva, O.V., Prokofyev, A.O., Nikolaeva, A.Y., Stroganova, T.A., 2015. Frequency of gamma oscillations in humans is modulated by velocity of visual motion. J. Neurophysiol. 114, 244–255.
Peiker, I., David, N., Schneider, T.R., Nolte, G., Schöttle, D., Engel, A.K., 2015. Perceptual integration deficits in autism spectrum disorders are associated with reduced interhemispheric gamma–band coherence. J. Neurosci. 35, 16352–16361.
Perry, G., Hamandi, K., Brindley, L.M., Muthukumaraswamy, S.D., Singh, K.D., 2013. The properties of induced gamma oscillations in human visual cortex show individual variability in their dependence on stimulus size. Neuroimage 68, 83–92.
Ray, S., Maunsell, J.H., 2010. Differences in gamma frequencies across visual cortex restrict their possible use in computation. Neuron 67, 885–896.
Roberts, M.J., Lowet, E., Brunet, N.M., Ter Wal, M., Tiesinga, P., Fries, P., De Weerd, P., 2013. Robust gamma coherence between macaque V1 and V2 by dynamic frequency matching. Neuron 78, 523–536.
Robson, S.E., Muthukumarawswamy, S.D., Evans, C.J., Shaw, A., Brealy, J., Davis, B., McNamara, G., Perry, G., Singh, K.D., 2015. Structural and neurochemical correlates of individual differences in gamma frequency oscillations in human visual cortex. J. Anat. 227, 409–417.
Schoffelen, J.M., Poort, J., Oostenveld, R., Fries, P., 2011. Selective movement preparation is subserved by selective increases in corticomuscular gamma–band coherence. J. Neurosci. 31, 6750–6758.
Schwarzkopf, D.S., Robertson, D.J., Song, C., Barnes, G.R., Rees, G., 2012. The frequency of visually induced γ–band oscillations depends on the size of early human visual cortex. J. Neurosci. 32, 1507–1512.
Singer, W., Gray, C.M., 1995. Visual feature integration and the temporal correlation hypothesis. Annu. Rev. Neurosci. 18, 555–586.
Stroganova, T.A., Butorina, A.V., Sysoeva, O.V., Prokofyev, A.O., Nikolaeva, A.Y., Tsetlin, M.M., Orekhova, E.V., 2015. Altered modulation of gamma oscillation frequency by speed of visual motion in children with autism spectrum disorders. J. Neurodev. Disord. 7, 21.
Swettenham, J.B., Muthukumaraswamy, S.D., Singh, K.D., 2009. Spectral properties of induced and evoked gamma oscillations in human early visual cortex to moving and stationary stimuli. J. Neurophysiol. 102, 1241–1253.
Thompson, P.M., Stein, J.L., Medland, S.E., Hibar, D.P., Vasquez, A.A., et al., 2014. The ENIGMA Consortium: large–scale collaborative analyses of neuroimaging and genetic data. Brain Imaging Behav 8, 153–182.
Tiesinga, P., Sejnowski, T.J., 2009. Cortical enlightenment: are attentional gamma oscillations driven by ING or PING? Neuron 63, 727–732.
Uhlhaas, P.J., Singer, W., 2006. Neural synchrony in brain disorders: relevance for cognitive dysfunctions and pathophysiology. Neuron 52, 155–168.
van Ede, F., van Pelt, S., Fries, P., Maris, E., 2015. Both ongoing alpha and visually induced gamma oscillations show reliable diversity in their across–site phase–relations. J. Neurophysiol. 113, 1556–1563.
van Pelt, S., Fries, P., 2013. Visual stimulus eccentricity affects human gamma peak frequency. Neuroimage 78, 439–447.
van Pelt, S., Boomsma, D.I., Fries, P., 2012. Magnetoencephalography in twins reveals a strong genetic determination of the peak frequency of visually induced gamma–band synchronization. J. Neurosci. 32, 3388–3392.
Van Veen, B.D., Van Drongelen, W., Yuchtman, M., Suzuki, A., 1997. Localization of brain electrical activity via linearly constrained minimum variance spatial filtering. IEEE Trans. Biomed. Eng. 44, 867–880.
Vinck, M.1, Womelsdorf, T., Buffalo, E.A., Desimone, R., Fries, P., 2013. Attentional modulation of cell–class–specific gamma–band synchronization in awake monkey area v4. Neuron 80, 1077–1089.
Whittington, M.A., Traub, R.D., Kopell, N., Ermentrout, B., Buhl, E.H., 2000. Inhibition–based rhythms: experimental and mathematical observations on network dynamics. Int. J. Psychophysiol. 38, 315–336.
Wyart, V., Tallon–Baudry, C., 2008. Neural dissociation between visual awareness and spatial attention. J. Neurosci. 28, 2667–2679.
Zhang, S., Xu, M., Kamigaki, T., Hoang Do, J.P., Chang, W.C., Jenvay, S., Miyamichi, K., Luo, L., Dan, Y., 2014. Selective attention. Long–range and local circuits for top–down modulation of visual cortex processing. Science 345, 660–665.